SCIENCE CHINA
Information Sciences

• **Supplementary File** •

Finite-time Bearing-only Formation of First-order Multi-agent Systems under Pinning Control

Chenjun Liu, Wei Zhu* & Fenglan Sun

Key Laboratory of Intelligent Analysis and Decision on Complex Systems,
Chongqing University of Posts and Telecommunications, Chongqing 400065, *China*

Appendix A Literature Review

The swarm phenomenon in nature inspired the development of multi-agent systems (MASs). They are made up of interacting agents that can perform complex tasks through mutual communication, collaboration, and competition. Formation control is one of hottest subjects in the field of MASs due to its wide applications in multiple vehicles formation [1], autonomous navigation [2], multi-manipulator collaborative assembly [3], and target encirclement [4]. The goal of formation is to build appropriate controllers to help MASs form and maintain desirable formation. Many scholars have concentrated on this critical issue by employing various agents' information, such as position [5, 6], distance [7, 8], bearing and so on.

Due to the translational and scaling invariance of bearing information, bearing-based formation control has received a lot of attention in recent years [9, 10]. Conveniently, obstacle avoidance can be accomplished via formation maneuver control [9, 11]. Bearing information may be gathered easily by a range of simple devices, such as passive sonars [12] and vision sensors [13], providing a viable solution for formation control in the case of a GPS-denied environment or lower cost. Moreover, a time-varying bearing formation based on persistently exciting can handle multiple real scenarios [14], including target encirclement and orbit maintenance.

Bearing-only formation control is referred to as a control scheme utilizing only bearing information, which has been designed for first-order continuous MASs [15], first-order discrete MASs [16], second-order MASs [17], and several kinds of robotic systems [18]. Meanwhile, many control structures, including leaderless control [15], leader-following control [19], and leader-first-following control [20], have been considered to solve the bearing-only formation problem. In a structure with the leader, the researchers have investigated the bearing-only control for stationary formation [16], tracking leader's constant velocity [21] and tracking leader's time-varying velocity [22], respectively. Moreover, some relevant results on undirected graphs [15–19, 21] and directed graphs [20, 22] are also included in the existing bearing-only formation research.

The finite-time control approach is a key tool due to better anti-interference and faster convergence. A finite-time controller can estimate the upper bound of the formation stabilization time in addition to stabilizing the formation more quickly [23]. The relative position information among agents must be obtained by using finite-time formation control strategies proposed in [24] and [25]. Two finite-time bearing-only controllers were designed in [26], which were intended as a symbolic or fractional power function. In the absence of a common global coordinate frame, Reference [27] studied an orientation estimation-based scheme to solve the static formation problem in finite time. However, the convergence time was related to the initial states. Then, the user-defined convergence time was explored for finite-time bearing-only formation control of heterogeneous robots presented in [28], where the control input was smooth. It is clear that this approach of [28] has a wide range of possible applications, but is now exclusively employed for stationary bearing-only formation.

Pinning control, which forms the desired formation by manipulating a few agents, is an efficient control for attaining formation. Using this approach, it is frequently possible to facilitate control for every node in large-scale networks. In [29], pinning control was adopted to study the formation control problem for MASs with nonlinear dynamics and fixed topology. Moreover, for nonlinear MASs with time-varying delay under directed switching topology, a pinning consensus criterion was put out in [30]. It is clear that only a fraction of agents have the availability of the reference state. A group consensus with pinning control for heterogeneous MASs was presented in [31]. In all of the aforementioned research, the relative position is the primary information transmission between agents, which may result in limited practical applications.

Appendix B Notations

$\|\cdot\|$ denotes the Euclidean norm of a vector or the spectral norm of a matrix. $\mathbf{0}_n = [0, \ldots, 0]^T$ and $\mathbf{1}_n = [1, \ldots, 1]^T$. For $y_i \in \mathbb{R}(i \in \{1, \ldots, n\})$, $\min_i\{y_i\}$ and $\max_i\{y_i\}$ denote the smallest and biggest one of them, respectively. For vectors $c_i \in \mathbb{R}^n$, $\mathrm{span}\{c_1, \ldots, c_n\}$ represents the linear span of these vectors. For a series of symmetric matrices $M_i \in \mathbb{R}^{m\times m}$, $\lambda_{\min}(M_i)$ is the minimum eigenvalue of M_i and $\mathrm{null}(M_i)$ is the null space of M_i. $\mathrm{diag}(M_1, \ldots, M_n)$ denotes the block-diagonal matrix with diagonal blocks $M_1, \ldots, M_n$. $\mathbb{R}_{>0}$ and $\mathbb{R}_{\geqslant 0}$ denote the sets of positive real numbers and non-negative real numbers. $f : \mathbb{R} \to \mathbb{R}_{\geqslant 0}$ and $\psi : \mathbb{R}_{\geqslant 0} \to \mathbb{R}_{>0}$ denote the mapping functions on different sets, respectively.

* Corresponding author (email: zhuwei@cqupt.edu.cn)

Appendix C Theory of Graph

Appendix C.1 Bearing Laplacian Matrix

Define the bearing Laplacian matrix $L \in \mathbb{R}^{dn \times dn}$ as

$$[L]_{ij} = \begin{cases} \mathbf{0}_{d\times d}, & i \neq j,\ (i,j) \notin E, \\ -P_{g^*_{ij}}, & i \neq j,\ (i,j) \in E, \\ \sum\limits_{k\in\mathcal{N}_i} P_{g^*_{ik}}, & i = j,\ i \in V. \end{cases}$$

For an undirected graph, $L \geqslant 0$ and $\mathrm{null}(L) \supseteq \mathrm{span}\{x^*, \mathbf{1}_n \otimes I_d\}$ [32]. L represents the topological structure of the network and the relative bearing between neighbors. The relationship between L and $\bar{H}$ is $L = \bar{H}^T \mathrm{diag}(P_{g_1}, \ldots, P_{g_s})\bar{H}$. For the leader-follower case, L can be decomposed as

$$L = \begin{bmatrix} L_{ll} & L_{lf} \\ L_{fl} & L_{ff} \end{bmatrix},$$

where $L_{ll} \in \mathbb{R}^{dn_l \times dn_l}$ and $L_{ff} \in \mathbb{R}^{dn_f \times dn_f}$. In this paper, $x^*_i(t)$ is uniquely determined by $x^*_f(t) = -L^{-1}_{ff} L_{fl} x_l(t)$ and $x^*_l(t) = x_l(t)$ [11].

Appendix C.2 Pinning Control Strategy

Based on the topological structure, the pinning matrix $D \in \mathbb{R}^{m\times n}$ of the graph G is defined as

$$d_{si} = \begin{cases} a_{si}, & (i,j) \in E_1 \text{ or } (i,j) \in E_2, \\ b_{si}, & (j,i) \in E_1 \text{ or } (j,i) \in E_2, \\ 0, & \text{others}, \end{cases}$$

where $a_{si} < 1$, $b_{si} > -1$, $E_1 = \{(i,j) \in \bar{E} | i \in V_l, j \in V_f\}$ and $E_2 = \{(i,j) \in \bar{E} | i \in V_f, j \in V_l\}$.

Then, the detailed pinning control strategy is as follows: Firstly, all leaders are selected as the pinning agents. Moreover, if the i-th agent for $i \in V_f$ needs to be pinned and $(i,j) \in E_2$, one has $h_{si} + a_{si} < 0$ and $h_{sj} + b_{sj} > 0$. Since the i-th and j-th agents are connected by the s-th edge, then the weights $|a_{si}|$ and $|b_{sj}|$ should be the same. This method guarantees the pinning control gain $|h_{si} + d_{si}| = |h_{sj} + d_{sj}| \neq 0$. Otherwise, the agent is not pinned, i.e., $|h_{si} + d_{si}| = |h_{sj} + d_{sj}| = 0$. Finally, the feasibility of this strategy is subsequently reflected in (D8) and (E14), where $\min_k\{1 + b_{ki}\} > 0$ is the necessary condition for stability.

Appendix D Preliminaries and Problem Formulation

Consider the following MAS with n_l leaders and n_f followers, which are described by single-integrator dynamics, i.e.,

$$\dot{x}_i(t) = u_i(t), \qquad i \in V, \tag{D1}$$

where $x_i(t)$, $u_i(t)$ are the position and control input of each agent, respectively.

Suppose that leaders move with constant velocity $\bar{v} = [\bar{v}_1, \ldots, \bar{v}_d]^T$. Define the position differences as $\varepsilon_i(t) = x_i(t) - x_i(t_0)$ and $\varepsilon^*_i(t) = x^*_i(t) - x^*_i(t_0)$ for all $i \in V$. Motivated by [17] and [33], the control input $u_i(t)$ for each follower is designed as

$$u_i(t) = \Big(\alpha + \gamma\frac{\dot{\varphi}(t)}{\varphi(t)}\Big)\Big[\sum_{j\in\mathcal{N}_i}(g_{ij}(t) - g^*_{ij}) + \sum_{j\in V_l} d_{si}(g_{ij}(t) - g^*_{ij})\Big] - o_i(\varepsilon_i(t) - \varepsilon^*_i(t)), \qquad i \in V_f, \tag{D2}$$

where α, γ, $o_i = \mathrm{diag}(o_{i1}, o_{i2}, \ldots, o_{id}) \in \mathbb{R}^{d\times d}$ are control gains. $\varphi : \mathbb{R}_{\geqslant 0} \to \mathbb{R}_{>0}$ is a function defined as

$$\varphi(t) = \begin{cases} (\frac{\Lambda - t_0}{\Lambda - t})^q, & t \in [t_0, \Lambda), \\ 1, & t \in [\Lambda, \infty), \end{cases} \tag{D3}$$

where $q \in \mathbb{R}_{>0}$ is the user-chosen parameter. The derivative of $\varphi(t)$ is

$$\dot{\varphi}(t) = \begin{cases} \frac{q(\frac{\Lambda - t_0}{\Lambda - t})^q}{\Lambda - t}, & t \in [t_0, \Lambda), \\ 0, & t \in [\Lambda, \infty), \end{cases} \tag{D4}$$

where the right-hand derivative of $\varphi(t)$ at $t = \Lambda$ is used as $\dot{\varphi}(\Lambda)$.

Apparently, $\varphi(t)$ satisfies the definition of function in the following lemma.

Lemma D1. [15] Suppose $f : \mathbb{R} \to \mathbb{R}_{\geqslant 0}$ is a continuously differentiable function. $\psi : \mathbb{R}_{\geqslant 0} \to \mathbb{R}_{>0}$ is a function that satisfies $\psi^{-\phi}(t_0) = 1$ for all $\phi \in \mathbb{R}_{>0}$, $\lim_{t\to\Lambda^-} \psi^{-\phi}(t) = 0$, and $\psi^{-\phi}(t)$ is monotonically decreasing on $[t_0, \Lambda)$, where $t_0 \in \mathbb{R}_{\geqslant 0}$ and $\Lambda > t_0$. If

$$\dot{f}(t) \leqslant -\varpi f(t) - \varrho\frac{\dot{\psi}}{\psi} f(t), \qquad t \in [t_0, \infty), \tag{D5}$$

where ϖ and ϱ are positive constants, then we conclude that

$$f(t) \begin{cases} \leqslant e^{-\varpi(t - t_0)}\psi^{-\varrho} f(t_0), & t \in [t_0, \Lambda), \\ = 0, & t \in [\Lambda, \infty). \end{cases} \tag{D6}$$

Then, using the control mechanism (D2), the compact form of MASs (D1) can be rewritten as

$$\dot{x}(t) = -\Big(\alpha + \gamma\frac{\dot{\varphi}}{\varphi}\Big)\begin{bmatrix}\mathbf{0}_{dn_l\times dn_l} & \mathbf{0}_{dn_l\times dn_f}\\ \mathbf{0}_{dn_f\times dn_l} & I_{dn_f}\end{bmatrix}(\bar{H}^T + \bar{D}^T)$$
$$(g(t) - g^*) + \begin{bmatrix}\mathbf{1}_{n_l}\otimes\bar{v}\\ \mathbf{0}_{dn_f}\end{bmatrix} - O(\varepsilon(t) - \varepsilon^*(t)), \tag{D7}$$

where $O = \mathrm{diag}(O_l, O_f) = \mathrm{diag}(o_1,\ldots,o_n)$, $\varepsilon(t) = [\varepsilon_l^T(t), \varepsilon_f^T(t)]^T = [\varepsilon_1^T(t),\ldots,\varepsilon_n^T(t)]^T$, and $\varepsilon^*(t)$ is the similar compact form.

Based on Lemmas 2 and 3 in [17], with mild revision, we have the following lemma.

Lemma D2. Suppose no agents coincide at any time. It holds that

$$x^T(\bar{H}^T + \bar{D}^T)(g - g^*) \geqslant \frac{\min_s\{1 + b_{si}\}\lambda_{\min}(L_{ff})}{2\max_s\|e_s\|}\|x - x^*\|^2, \tag{D8}$$

$$(x^*)^T(\bar{H}^T + \bar{D}^T)(g - g^*) \leqslant 0, \tag{D9}$$

where the equality of (D9) holds if and only if $g = g^*$.

Assumption 1. [17] The desired formation (G, x^*) can be uniquely determined by the bearing vectors $\{g_{ij}^*\}_{(i,j)\in E}$ and the leaders' positions $\{x_i^*\}_{i\in V_l}$ if and only if $L_{ff} > 0$.

Assumption 2. [30] Suppose G_f is the graph composed by followers, which has r disjoint strong components namely $G_1,\ldots,G_r$ with $V(G_i)\bigcap V(G_j) = \emptyset$, $i,j = 1,\ldots,r$, $i\neq j$, and $\bigcup_{i=1}^r V(G_i)\subseteq V(G)$. $V(G_i)$ denotes the vertex set of the i-th strong components. If $\bigcup_{i=1}^r V(G_i)\subset V(G)$, assume that each vertex in $V(G)\backslash\bigcup_{i=1}^r V(G_i)$ is reachable from at least one vertex in $\bigcup_{i=1}^r V(G_i)$.

Appendix E The Proofs of Main Results

Let the initial states be $x(t_0) = [(x_l^*(t_0))^T, x_f^T(t_0)]$ and $\dot{x}(t_0) = [(v_l^*(t_0))^T, v_f^T(t_0)] = [\mathbf{1}_{n_l}\otimes\bar{v}, v_f^T(t_0)]$. Then, the position error is $\delta_i(t) = x_i(t) - x_i^*(t) = [\delta_{i1}^T(t),\ldots,\delta_{id}^T(t)]^T$ and $\delta(t) = [\delta_l^T(t), \delta_f^T(t)] = [\delta_1^T(t),\ldots,\delta_n^T(t)]^T$.

Appendix E.1 Collision Avoidance

Below is a demonstration of the sufficient condition for collision avoidance.

Theorem 1. Under Assumption 1, if

$$\|\delta(t)\| \leqslant \theta := \frac{1}{\sqrt{2}}\Big(\min_{i,j\in V}\|x_i^* - x_j^*\| - \xi\Big), \tag{E1}$$

for any $\xi\in(0, \min_{i,j\in V}\|x_i^* - x_j^*\|)$, then $\|x_i(t) - x_j(t)\| \geqslant \xi$ for any $i,j\in V$ and $t > t_0$. Namely, a collision-free path can be produced for each agent.

Furthermore, if $\|\delta(t)\| \leqslant \|\delta(t_0)\|$ for any $t > t_0$, the condition can be replaced by $\|\delta(t_0)\| \leqslant \theta$.

Proof. Notice that

$$x_i(t) - x_j(t) = (x_i^*(t) - x_j^*(t)) + (x_i(t) - x_i^*(t)) - (x_j(t) - x_j^*(t)). \tag{E2}$$

It holds that

$$\begin{aligned}\|x_i(t) - x_j(t)\| \geqslant & \|x_i^*(t) - x_j^*(t)\| - \|x_i(t) - x_i^*(t)\| - \|x_j(t) - x_j^*(t)\|\\ \geqslant & \|x_i^*(t) - x_j^*(t)\| - \sqrt{2\|x_i(t) - x_i^*(t)\|^2 + 2\|x_j(t) - x_j^*(t)\|^2}\\ \geqslant & \|x_i^*(t) - x_j^*(t)\| - \sqrt{2\sum_{k=1}^n\|x_k(t) - x_k^*(t)\|^2}\\ = & \|x_i^*(t) - x_j^*(t)\| - \sqrt{2}\|x(t) - x^*(t)\|\\ = & \|x_i^*(t) - x_j^*(t)\| - \sqrt{2}\|\delta(t)\|.\end{aligned} \tag{E3}$$

Since $\|\delta(t)\| \leqslant \theta$, we have $\|x_i(t) - x_j(t)\| \geqslant \xi$ for any $i,j\in V$ and $t > t_0$, which implies that there is a collision-free path for each agent.

Appendix E.2 Formation Stabilization

Theorem 2. Suppose Assumptions 1 and 2 hold. Consider the first-order MAS (D1) with the control input (D2). If

$$o_w = \mathrm{diag}\Big(\frac{\bar{v}_1}{\delta_{w1}(t_0)},\ldots,\frac{\bar{v}_d}{\delta_{wd}(t_0)}\Big), \tag{E4}$$

where $\frac{\bar{v}_k}{\delta_{wk}(t_0)} > 0$, $w\in\{n_l + 1,\ldots,n\}$ and $k\in\{1,\ldots,d\}$, then x converges to x^* as $t\to\Lambda$ and $x = x^*$ for $t\geqslant\Lambda$. Moreover, the control input $u_f(t) = [u_{n_l+1}^T(t),\ldots,u_n^T(t)]^T$ holds C^1 smooth and bounded for $[t_0, +\infty)$ with the condition that

$$q\gamma > \frac{4\|\bar{H}\|(\|\delta(t_0)\| + \|\widetilde{x}^*\|)}{\min_s\{1 + b_{si}\}\lambda_{\min}(L_{ff})}. \tag{E5}$$

Proof. Note that $v^* = [(v_1^*)^T, \ldots, (v_{n_l}^*)^T, (v_{n_l+1}^*)^T, \ldots, (v_n^*)^T]^T = [(v_l^*)^T, (v_f^*)^T]^T = \mathbf{1}_n \otimes \bar{v}$. Since $\dot{x}^*(t) = v^*$ and $x_l(t) = x_l^*(t)$, we have $\dot{\delta}(t) = \dot{x}(t) - v^*$ and $\delta(t) = [\mathbf{0}_{dn_l}^T, \delta_f^T(t)]^T$.

Consider the Lyapunov function

$$V = \frac{1}{2}\|\delta(t)\|^2. \tag{E6}$$

Calculating the derivative of V along the solution of equation (D7), we have

$$\begin{aligned}\dot{V} =& \delta^T(t)\dot{\delta}(t)\\ =& \delta^T(t)\left\{-\Big(\alpha+\gamma\frac{\dot{\varphi}}{\varphi}\Big)\begin{bmatrix}\mathbf{0}_{dn_l\times dn_l} & \mathbf{0}_{dn_l\times dn_f}\\ \mathbf{0}_{dn_f\times dn_l} & I_{dn_f}\end{bmatrix}(\bar{H}^T+\bar{D}^T)(g(t)-g^*)+\begin{bmatrix}\mathbf{1}_{n_l}\otimes u_0\\ \mathbf{0}_{dn_f}\end{bmatrix}-O(\varepsilon(t)-\varepsilon^*(t))-v^*\right\}\\ =& -(\alpha+\gamma\frac{\dot{\varphi}}{\varphi})\delta^T(t)(\bar{H}^T+\bar{D}^T)(g(t)-g^*)-\delta^T(t)O(\varepsilon(t)-\varepsilon^*(t))-\delta^T(t)v^*.\end{aligned} \tag{E7}$$

Let

$$\dot{V}_1 = -\Big(\alpha+\gamma\frac{\dot{\varphi}}{\varphi}\Big)\delta^T(t)(\bar{H}^T+\bar{D}^T)(g(t)-g^*) \tag{E8}$$

and

$$\dot{V}_2 = -\delta^T(t)O(\varepsilon(t)-\varepsilon^*(t))-\delta^T(t)v^*. \tag{E9}$$

By the definition of edge e_s, one has

$$\begin{aligned}\max_s\|e_s(t)\| \leqslant \|e(t)\| &= \|\bar{H}x(t)-\bar{H}x^*(t)+\bar{H}x^*(t)\|\\ &= \|\bar{H}\delta(t)+\bar{H}x^*(t)-\bar{H}\bar{x}^*(t)\|\\ &\leqslant \|\bar{H}\|\|\delta(t)+\tilde{x}^*\|\\ &\leqslant \|\bar{H}\|(\|\delta(t)\|+\|\tilde{x}^*\|),\end{aligned} \tag{E10}$$

where $\bar{x}^*(t) = \mathbf{1}_n\otimes\big((\sum_{i=1}^n x_i^*(t))/n\big)$, $(\sum_{i=1}^n x_i^*(t))/n$ denotes the centroid of the desired formation and $\tilde{x}^*$ is time-invariant.

In terms of (D8), (D9), (E10) and (D3), we obtain that

$$\begin{aligned}\dot{V}_1 &= -\Big(\alpha+\gamma\frac{\dot{\varphi}}{\varphi}\Big)(x^T(t)-(x^*(t))^T)(\bar{H}^T+\bar{D}^T)(g(t)-g^*)\\ &\leqslant -\Big(\alpha+\gamma\frac{\dot{\varphi}}{\varphi}\Big)x^T(t)(\bar{H}^T+\bar{D}^T)(g(t)-g^*)\\ &\leqslant -\Big(\alpha+\gamma\frac{\dot{\varphi}}{\varphi}\Big)\frac{\min_s\{1+b_{si}\}\lambda_{\min}(L_{ff})}{2\max_s\|e_s\|}\|\delta(t)\|^2\\ &\leqslant -\Big(\alpha+\gamma\frac{\dot{\varphi}}{\varphi}\Big)\frac{\min_s\{1+b_{si}\}\lambda_{\min}(L_{ff})}{\|\bar{H}\|(\|\delta(t)\|+\|\widetilde{x}^*\|)}V\leqslant 0.\end{aligned} \tag{E11}$$

On the other hand, we have

$$\begin{aligned}\dot{V}_2 &= -\delta^T(t)O\delta(t)+\delta^T(t)O\delta(t_0)-\delta^T(t)v^*\\ &= -\delta^T(t)O\delta(t)+\delta^T(t)\big[O\delta(t_0)-v^*\big]\\ &= -\delta_f^T(t)O_f\delta_f(t)+\delta_f^T(t)\big[O_f\delta_f(t_0)-v_f^*\big]\\ &\leqslant -2\lambda_{\min}(O_f)V+\|\delta(t)\|\|O_f\delta_f(t_0)-v_f^*\|.\end{aligned} \tag{E12}$$

By the condition that $o_w = \mathrm{diag}(\frac{\bar{v}_1}{\delta_{w1}(t_0)},\ldots,\frac{\bar{v}_d}{\delta_{wd}(t_0)})$, where $\frac{\bar{v}_k}{\delta_{wk}(t_0)} > 0$ and $w\in\{n_l+1,\ldots,n\}$, we have $\|O_f\delta_f(t_0)-v_f^*(t)\| = 0$ and O_f is a positive definite matrix. Thus, by (E12), we can obtain that

$$\dot{V}_2 \leqslant -2\lambda_{\min_f}(O_f)V. \tag{E13}$$

Combining (E11) with (E13), it holds that $\dot{V}\leqslant 0$, which implies that $\|\delta(t)\|\leqslant\|\delta(t_0)\|$. Then, we have

$$\dot{V}\leqslant -\Big(\alpha+\gamma\frac{\dot{\varphi}}{\varphi}\Big)\frac{\min_s\{1+b_{si}\}\lambda_{\min}(L_{ff})}{\|\bar{H}\|(\|\delta(t_0)\|+\|\widetilde{x}^*\|)}V-2\lambda_{\min}(O_f)V := -\tilde{\alpha}V-\tilde{\gamma}\frac{\dot{\varphi}}{\varphi}V, \tag{E14}$$

where

$$\begin{aligned}\tilde{\alpha} =& \frac{\alpha\min_s\{1+b_{si}\}\lambda_{\min}(L_{ff})}{\|\bar{H}\|(\|\delta(t_0)\|+\|\widetilde{x}^*\|)}+2\lambda_{\min}(O_f)>0,\\ \tilde{\gamma} =& \frac{\gamma\min_s\{1+b_{si}\}\lambda_{\min}(L_{ff})}{\|\bar{H}\|(\|\delta(t_0)\|+\|\widetilde{x}^*\|)}>0.\end{aligned}$$

In terms of Lemma D1, we obtain that

$$\|\delta(t)\|\begin{cases}\leqslant\sqrt{e^{-\tilde{\alpha}(t-t_0)}\varphi^{-\tilde{\gamma}}}\|\delta(t_0)\|, & t\in[t_0,\Lambda),\\ =0, & t\in[\Lambda,+\infty).\end{cases} \tag{E15}$$

Hence, $x \to x^*$ in finite time, which implies the desired formation is achieved.

Next, it is proved that u_f holds C^1 smooth and bounded for $[t_0, +\infty)$.

Since g_s is the unit vector and (E1), we have

$$\begin{aligned}\|e(t)-e^*\|^2 =& \sum_{s=1}^{m}\left(\|e_s(t)\|^2+\|e_s^*\|^2-2\|e_s(t)\|\|e_s^*\|g_s^T(t)g_s^*\right)\\ \geqslant& \sum_{s=1}^{m}\left(2\|e_s(t)\|\|e_s^*\|-2\|e_s(t)\|\|e_s^*\|g_s^T(t)g_s^*\right)\\ \geqslant& \sum_{s=1}^{m}2\xi^2(1-g_s^T(t)g_s^*)\\ =&\xi^2\|g(t)-g^*\|^2. \end{aligned}\tag{E16}$$

It follows from (E16) that

$$\|g(t)-g^*\| \leqslant \frac{1}{\xi}\|e(t)-e^*\| = \frac{1}{\xi}\|\bar{H}\delta(t)\|.\tag{E17}$$

From (E15) and (E17), we have

$$\|g(t)-g^*\| \leqslant \frac{\|\bar{H}\|e^{-\frac{\tilde{\alpha}}{2}(t-t_0)}}{\xi}\varphi^{-\frac{\tilde{\gamma}}{2}}\|\delta(t_0)\|\tag{E18}$$

for $t \in [t_0, \Lambda)$ and $\|g(t)-g^*\| = 0$ for $t \in [\Lambda, +\infty)$.

It can be obtained from (E5) that $q\tilde{\gamma} > 2$. Then, combining the fact that $\frac{\dot{\varphi}}{\varphi} = (\frac{q}{\Lambda-t_0})\varphi^{\frac{1}{q}}$, we have

$$\|\frac{\dot{\varphi}}{\varphi}(g(t)-g^*)\| \leqslant \frac{q\|\bar{H}\|e^{-\frac{\tilde{\alpha}}{2}(t-t_0)}}{\xi(\Lambda-t_0)}\varphi^{-(\frac{\tilde{\gamma}}{2}-\frac{1}{q})}\|\delta(t_0)\|,\tag{E19}$$

for $t \in [t_0, \Lambda)$ and $\|\frac{\dot{\varphi}}{\varphi}(g(t)-g^*)\| = 0$ for $t \in [\Lambda, +\infty)$.

By (E4) and (E15), we obtain that

$$\begin{aligned}\|O(\varepsilon(t)-\varepsilon^*(t))\| \leqslant& \|O\delta(t)\|+\|O\delta(t_0)\|\\ \leqslant& e^{-\frac{\tilde{\alpha}}{2}(t-t_0)}\varphi^{-\frac{\tilde{\gamma}}{2}}\|O_f\|\|\delta(t_0)\|+\|\mathbf{1}_{n_f}\otimes u_0\|\end{aligned}\tag{E20}$$

for $t \in [t_0, \Lambda)$ and $\|O(\varepsilon(t)-\varepsilon^*(t))\| = \|\mathbf{1}_{n_f}\otimes u_0\|$ for $t \in [\Lambda, +\infty)$.

Then, we have

$$\|u_f(t)\| \leqslant \Big(\alpha+\gamma\frac{\dot{\varphi}}{\varphi}\Big)\|\bar{H}+\bar{D}\|\|g(t)-g^*\|+\|O_f(\varepsilon(t)-\varepsilon^*(t))\|.\tag{E21}$$

By (E18), (E19) and (E20), we conclude that

$$\lim_{t\to\Lambda^-}\|u_f(t)\| = \|\mathbf{1}_{n_f}\otimes u_0\|\tag{E22}$$

and $\|u_f(t)\| = \|\mathbf{1}_{n_f}\otimes u_0\|$ for $t \in [\Lambda, +\infty)$, which implies that $u_f(t)$ is continuous and bounded for $[t_0, +\infty)$.

From (D7) and (E4), we have

$$\begin{aligned}\bar{H}\dot{x}(t) =& -\Big(\alpha+\gamma\frac{\dot{\varphi}}{\varphi}\Big)\bar{H}\begin{bmatrix}\mathbf{0}_{dn_l\times dn_l} & \mathbf{0}_{dn_l\times dn_f}\\ \mathbf{0}_{dn_f\times dn_l} & I_{dn_f}\end{bmatrix}(\bar{H}^T+\bar{D}^T)(g(t)-g^*)-\bar{H}O\delta(t)+\bar{H}O\delta(t_0)+\bar{H}\begin{bmatrix}\mathbf{1}_{n_l}\otimes u_0\\ \mathbf{0}_{dn_f}\end{bmatrix}\\ =& -\Big(\alpha+\gamma\frac{\dot{\varphi}}{\varphi}\Big)\bar{H}\begin{bmatrix}\mathbf{0}_{dn_l\times dn_l} & \mathbf{0}_{dn_l\times dn_f}\\ \mathbf{0}_{dn_f\times dn_l} & I_{dn_f}\end{bmatrix}(\bar{H}^T+\bar{D}^T)(g(t)-g^*)-\bar{H}O\delta(t)+\bar{H}(\mathbf{1}_n\otimes u_0)\\ =& -\Big(\alpha+\gamma\frac{\dot{\varphi}}{\varphi}\Big)\bar{H}\begin{bmatrix}\mathbf{0}_{dn_l\times dn_l} & \mathbf{0}_{dn_l\times dn_f}\\ \mathbf{0}_{dn_f\times dn_l} & I_{dn_f}\end{bmatrix}(\bar{H}^T+\bar{D}^T)(g(t)-g^*)-\bar{H}O\delta(t).\end{aligned}\tag{E23}$$

Let us calculate the derivative of $u_f(t)$ as follows

$$\begin{aligned}\|\dot{u}_f(t)\| \leqslant& \Big(\alpha+\gamma\frac{\dot{\varphi}}{\varphi}\Big)\|\bar{H}+\bar{D}\|\|\Gamma\Big(\frac{P_{g_s}}{\|e_s\|}\Big)\|\|\bar{H}\dot{x}(t)\|+\frac{\gamma q\|\bar{H}+\bar{D}\|}{(\Lambda-t_0)^2}\varphi^{\frac{2}{q}}\|g(t)-g^*\|+\|O_f(\dot{\varepsilon}_f(t)-\dot{\varepsilon}_f^*(t))\|\\ \leqslant& \Big(\alpha+\gamma\frac{\dot{\varphi}}{\varphi}\Big)^2\|\bar{H}+\bar{D}\|^2\|\bar{H}\|\|\Gamma\Big(\frac{P_{g_s}}{\|e_s\|}\Big)\|\|g(t)-g^*\|+\Big(\alpha+\gamma\frac{\dot{\varphi}}{\varphi}\Big)\|\bar{H}+\bar{D}\|\|\bar{H}O\|\|\Gamma\Big(\frac{P_{g_s}}{\|e_s\|}\Big)\|\|\delta(t)\|\\ &+\frac{\gamma q\|\bar{H}+\bar{D}\|}{(\Lambda-t_0)^2}\varphi^{\frac{2}{q}}\|g(t)-g^*\|+\|O_f(\dot{\varepsilon}_f(t)-\dot{\varepsilon}_f^*(t))\|,\end{aligned}\tag{E24}$$

where $\Gamma\Big(\frac{P_{g_s}}{\|e_s\|}\Big)$ denotes a partitioned diagonal matrix, which is composed of $\frac{P_{g_s}}{\|e_s\|}$ for $s \in \{1, ..., m\}$. Since $\Gamma\Big(\frac{P_{g_s}}{\|e_s\|}\Big)$ is bounded, there exist positive constants Φ_1, Φ_2 such that $\|\bar{H}+\bar{D}\|^2\|\bar{H}\|\|\Gamma\Big(\frac{P_{g_s}}{\|e_s\|}\Big)\| < \Phi_1$, $\|\bar{H}+\bar{D}\|\|\bar{H}O\|\|\Gamma\Big(\frac{P_{g_s}}{\|e_s\|}\Big)\| < \Phi_2$. Combined with $\Phi_3 = \frac{\gamma q\|\bar{H}+\bar{D}\|}{(\Lambda - t_0)^2}$, we obtain that

$$\begin{aligned}\|\dot{u}_f(t)\| \leqslant & \Big(\alpha + \gamma\frac{\dot{\varphi}}{\varphi}\Big)^2\Phi_1\|g(t)-g^*\| + \Big(\alpha + \gamma\frac{\dot{\varphi}}{\varphi}\Big)\Phi_2\|\delta(t)\| + \Phi_3\varphi^{\frac{2}{q}}\|g(t)-g^*\| \\ & + \|O_f(\dot{\varepsilon}_f(t) - \dot{\varepsilon}_f^*(t))\|, \end{aligned} \tag{E25}$$

Since

$$\Big(\alpha + \gamma\frac{\dot{\varphi}}{\varphi}\Big)^2 = \alpha^2 + \frac{2q\alpha\gamma}{\Lambda - t_0}\varphi^{\frac{1}{q}} + \Big(\frac{q\gamma}{\Lambda - t_0}\Big)^2\varphi^{\frac{2}{q}}, \tag{E26}$$

we obtain that

$$\begin{aligned}\|\dot{u}_f(t)\| \leqslant & \alpha^2\Phi_1\|g(t)-g^*\| + \frac{2q\alpha\gamma}{\Lambda - t_0}\Phi_1\varphi^{\frac{1}{q}}\|g(t)-g^*\| + \Big[\Big(\frac{q\gamma}{\Lambda - t_0}\Big)^2\Phi_1 + \Phi_3\Big]\varphi^{\frac{2}{q}}\|g(t)-g^*\| \\ & + \alpha\Phi_2\|\delta(t)\| + \frac{q\gamma}{\Lambda - t_0}\Phi_2\varphi^{\frac{1}{q}}\|\delta(t)\| + \|O_f u_f(t)\| + \|O_f(\mathbf{1}_{n_f}\otimes u_0)\|. \end{aligned} \tag{E27}$$

Based on the condition (E5), one has $q\bar{\gamma} > 4$. Then, by (E15), (E18), (E19) and (E20), we conclude that

$$\lim_{t\to\Lambda^-}\|\dot{u}_f(t)\| = 2\|O_f\|\|\mathbf{1}_{n_f}\otimes u_0\|. \tag{E28}$$

and $\|\dot{u}_f(t)\| = 2\|O_f\|\|\mathbf{1}_{n_f}\otimes u_0\|$ for $t \in [\Lambda, +\infty)$.

Therefore, if condition (E5) is satisfied, the control input u_f holds C^1 smooth and bounded for $[t_0, +\infty)$.

Remark 1. The control gain parameter O is designed based on the system environment, including the desired velocity and the initial positions. Due to the desired formation being fixed, the desired velocity of the follower is equal to the desired velocity of the leader. Thus, the follower should be aware of the leader's control input.

Appendix F Numerical Example

In this appendix, numerical simulation examples are presented to illustrated the effectiveness of the theoretical results.

Appendix F.1 Example 1

To illustrate that $\|\delta(t_0)\| \leqslant \theta$ is only a sufficient condition, the MAS with two leaders and seven followers is considered in the numerical example. The initial positions of leaders and followers are described in Figure F1. The desired positions at initial time are shown in Figure F2. By the definition of the undirected graph with an orientation, the edge set can be denoted as $\bar{E} = \{(1,2),(2,3),(3,4),(4,5),(5,6),(6,1),(1,7),(2,7),(3,7),(4,7),(5,7),(6,7),(6,8),(5,8),(4,9),(3,9)\}$, which corresponds to e_s for $s = \{1, ..., 16\}$. Then, the corresponding desired formation be $g^* = [(g_1^*)^T, (g_2^*)^T, (g_3^*)^T, (g_4^*)^T, (g_5^*)^T, (g_6^*)^T, (g_7^*)^T, (g_8^*)^T, (g_9^*)^T, (g_{10}^*)^T, (g_{11}^*)^T, (g_{12}^*)^T, (g_{13}^*)^T, (g_{14}^*)^T, (g_{15}^*)^T, (g_{16}^*)^T]^T = [-1, 0, -0.5, -0.866, 0.5, -0.866, 1, 0, 0.5, 0.866, -0.5, 0.866, -0.5, -0.866, 0.5, -0.866, 1, 0, 0.5, 0.866, -0.5, 0.866, -1, 0, 0.5, -0.866, 1, 0, -1, 0, -0.5, -0.866]^T$.

Let $\alpha = \gamma = 25$, $\Lambda = 15$, $q = 2$, $t_0 = 0$, $\bar{v} = [0.5, 0.5]^T$, and $o_1 = o_2 = \text{diag}(0, 0)$. Then, $\varphi(t) = 225/(15-t)^2$ on $[0, 15)$ and $\varphi(t) = 1$ on $[15, +\infty)$. Let the pinning matrix $[D]_{22} = -1$, $[D]_{23} = 1$, $[D]_{61} = 1$, $[D]_{66} = -1$, $[D]_{71} = -1$, $[D]_{77} = 1$, $[D]_{82} = -1$ and $[D]_{87} = 1$, implying the agents $2, 6, 7$ can obtain the information of leader 1 and the agents $1, 3, 7$ can obtain that of leader 2. Also, the pinning weights are all 2. Let $o_3 = \text{diag}(0.0833, 0.2887)$, $o_4 = \text{diag}(0.5000, 0.1443)$, $o_5 = \text{diag}(0.5000, 0.0481)$, $o_6 = \text{diag}(0.5000, 0.1443)$, $o_7 = \text{diag}(0.0833, 0.0361)$, $o_8 = \text{diag}(0.0833, 0.1443)$, and $o_9 = \text{diag}(0.2500, 0.2887)$, we have $\|O_f\delta_f(0) - v_f^*\| = 0$.

Based on the given initial positions and the desired initial positions, we obtain that $\|\delta(0)\| = 21.38$ and $\theta = 4.23 - (1/\sqrt{2})\xi$, where $\xi \in (0, 6)$. It's clear that $\|\delta(0)\|$ is far greater than θ. But the simulation results presented in Figures F3-F6 show that the tracking bearing-only formation is achieved with no collision between agents.

Appendix F.2 Example 2

Consider the MAS with two leaders and five followers and the network topology among them is shown in Figure F7. It clearly satisfies the uniqueness of bearing-only formation in Assumption 1 and the pinning condition in Assumption 2.

The initial positions of leaders are $x_1 = [2, \sqrt{3}]^T$ and $x_2 = [8, \sqrt{3}]^T$. By the definition of the undirected graph with an orientation, the edge set can be denoted as $\bar{E} = \{(1,2),(2,3),(3,4),(4,5),(5,6),(6,1),(1,7),(2,7),(3,7),(4,7),(5,7),(6,7)\}$, which corresponds to e_s for $s = \{1, ..., 12\}$. Let the corresponding desired formation be $g^* = [(g_1^*)^T, (g_2^*)^T, (g_3^*)^T, (g_4^*)^T, (g_5^*)^T, (g_6^*)^T, (g_7^*)^T, (g_8^*)^T, (g_9^*)^T, (g_{10}^*)^T, (g_{11}^*)^T, (g_{12}^*)^T]^T = [-1, 0, -0.5, -0.866, 0.5, -0.866, 1, 0, 0.5, 0.866, -0.5, 0.866, -0.5, -0.866, 0.5, -0.866, 1, 0, 0.5, 0.866, -0.5, 0.866, -1, 0]^T$, which is presented in Figure F8.

Let $\alpha = \gamma = 24$, $\Lambda = 5$, $q = 2$, $t_0 = 0$, $\bar{v} = [0.5, 0.5]^T$, and $o_1 = o_2 = \text{diag}(0, 0)$. Then, $\varphi(t) = 25/(5-t)^2$ on $[0, 5)$ and $\varphi(t) = 1$ on $[5, +\infty)$. The initial positions of followers are $x_3 = [12, 5\sqrt{3}]^T$, $x_4 = [9, 8\sqrt{3}]^T$, $x_5 = [3, 8\sqrt{3}]^T$, $x_6 = [0, 5\sqrt{3}]^T$ and $x_7 = [6, 5\sqrt{3}]^T$. The followers' initial velocity is zero and the leaders' initial velocity is the desired velocity $\bar{v}$. Based on the given initial positions and the desired formation, we obtain that $\|\delta(0)\| = 4$ and $\theta = 4.23 - (1/\sqrt{2})\xi$, where $\xi \in (0, 6)$.

Let the pinning matrix $[D]_{22} = -1$, $[D]_{23} = 1$, $[D]_{61} = 1$, $[D]_{66} = -1$, $[D]_{71} = -1$, $[D]_{77} = 1$, $[D]_{82} = -1$ and $[D]_{87} = 1$, implying the agents $2, 6, 7$ can obtain the information of leader 1 and the agents $1, 3, 7$ can obtain that of leader 2. Also, the pinning weights are all 2. Let $o_3 = \text{diag}(0.1250, 0.0722)$, $o_4 = \text{diag}(0.1667, 0.0962)$, $o_5 = \text{diag}(0.1667, 0.0962)$, $o_6 = \text{diag}(0.1250, 0.0722)$ and $o_7 = \text{diag}(0.0625, 0.0361)$, we have $\|O_f\delta_f(0) - v_f^*\| = 0$. Thus, by Theorem 1 and Theorem 2, the tracking bearing-only formation can be achieved asymptotically with no collision in finite time Λ.

Figures F9 and F10 illustrate that the bearing error and the velocity error converge to 0 in $\Lambda = 5$ s. It can be seen from Figure F11 that the minimum distance between agents is not zero, ie., there will be no collision between agents. In Figure F12, the trajectory of MASs from $t = 0$ s to $t = 20$ s is presented.

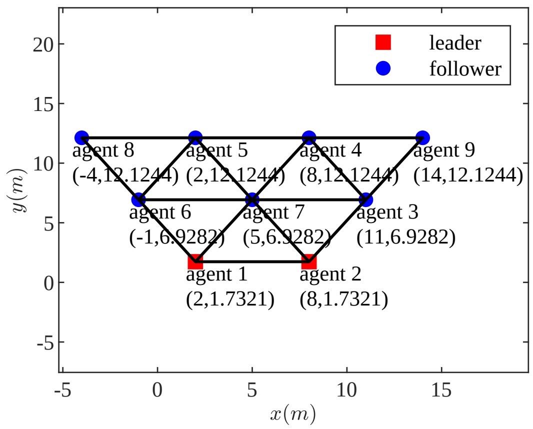

Figure F1 Desired positions at $t = 0$ s in Example 1.

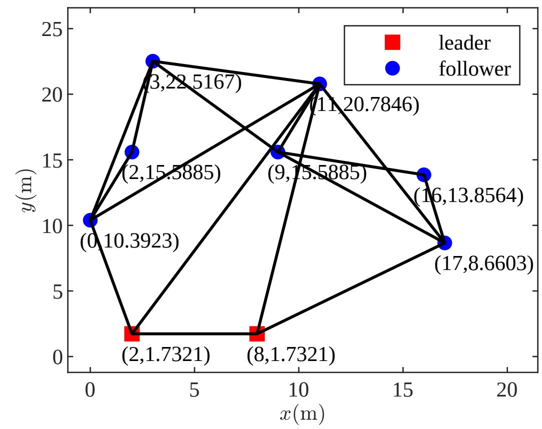

Figure F2 Initial positions at $t = 0$ s in Example 1.

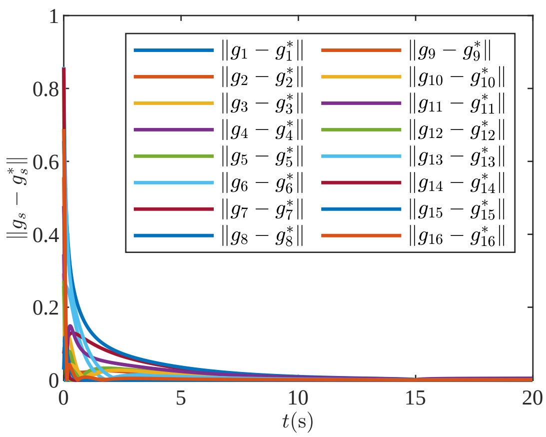

Figure F3 Bearing error $\|g_s - g_s^*\|$ of MASs in Example 1.

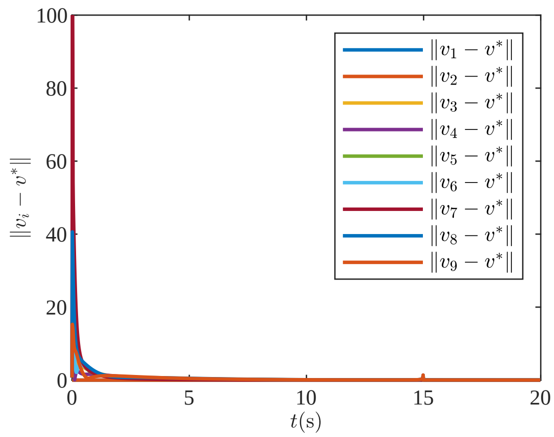

Figure F4 Velocity error $\|v_i - v^*\|$ of MASs in Example 1.

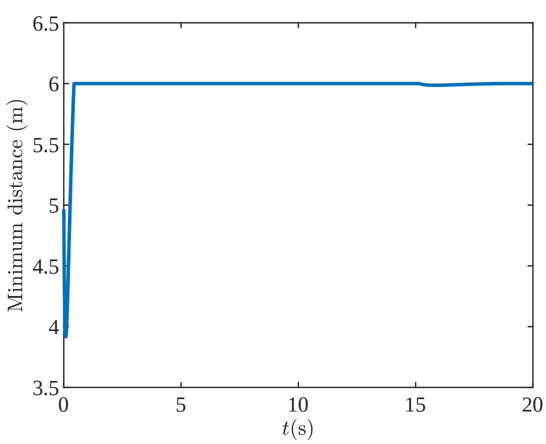

Figure F5 The minimum distance of agents in Example 1.

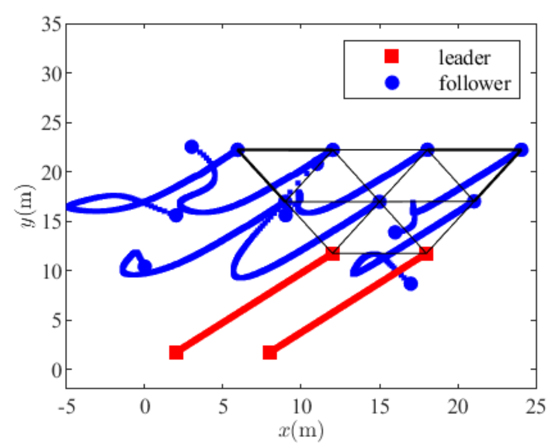

Figure F6 The evolution trajectory of MASs in Example 1.

Appendix F.3 Example 3

Consider the MAS (D1) under the formation control scheme for each follower:

$$u_i(t) = \alpha\Big[\sum_{j\in\mathcal{N}_i}(g_{ij}(t) - g_{ij}^*) + \sum_{j\in V_l} d_{si}(g_{ij}(t) - g_{ij}^*)\Big] + \alpha_2\int_0^t\Big[\sum_{j\in\mathcal{N}_i}(g_{ij}(\tau) - g_{ij}^*) + \sum_{j\in V_l} d_{si}(g_{ij}(\tau) - g_{ij}^*)\Big]d\tau, \qquad i \in V_f, \quad \text{(F1)}$$

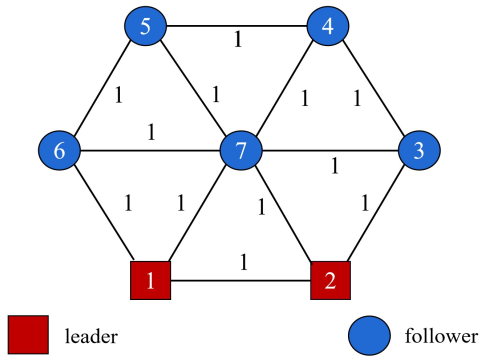

Figure F7 The network topology of MASs in Examples 2-3.

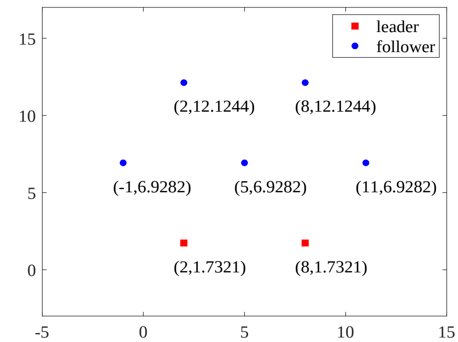

Figure F8 Desired formation at $t = 0$ s in Examples 2-3.

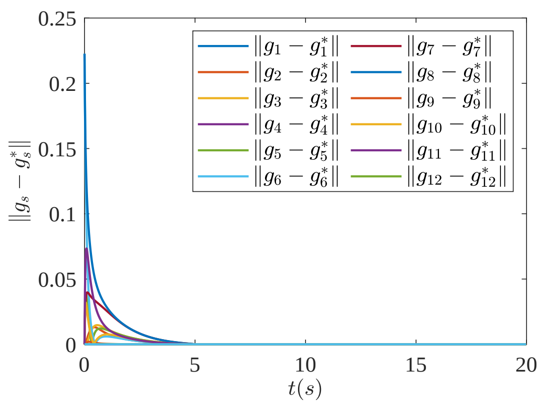

Figure F9 Bearing error $\|g_s - g_s^*\|$ of MASs in Example 2.

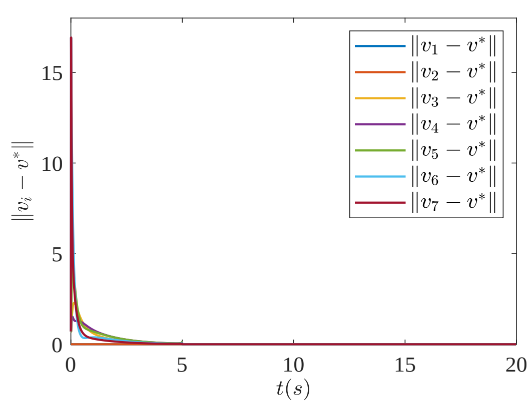

Figure F10 Velocity error $\|v_i - v^*\|$ of MASs in Example 2.

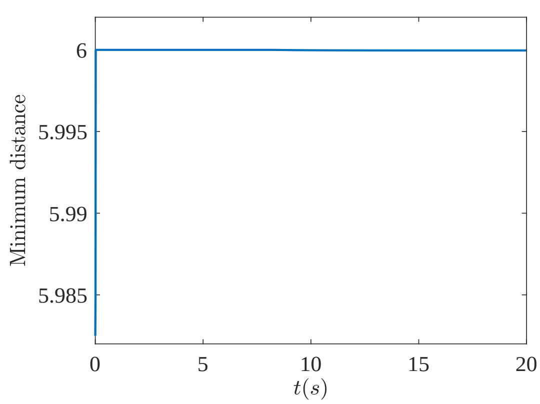

Figure F11 The minimum distance of agents in Example 2.

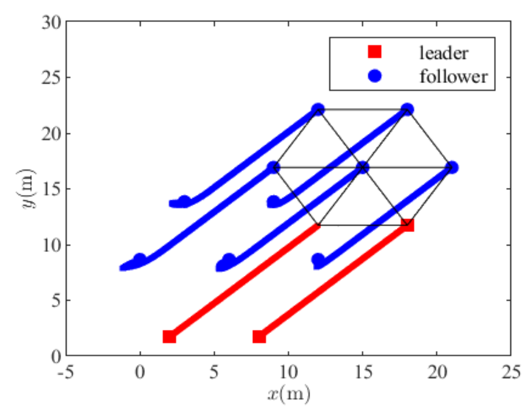

Figure F12 The evolution trajectory of MASs in Example 2.

which is similar to the control scheme proposed in [17] for the leader with constant velocity. Combining the proof of Theorem 2 in [17] and the matrix D proposed in this paper, it is obvious that the above system is stable by setting $V = x^T(\bar{H}^T + \bar{D}^T)(g - g^*)$, which is omitted here.

Then, let $\alpha_2 = 1$. To compare the control scheme (F1) with our finite-time control scheme (D2), Figures F13 and F14 depict the bearing error of the MAS with the same other parameters and initial states as in Example 2. It can be seen from Figure F13 that the MAS converges to 0 at about $t = 8$ s, but this instant cannot be determined in advance. However, under the finite-time control scheme (D2), Figures F14 and F9 show the bearing error under the condition $\Lambda = 2$ and $\Lambda = 5$, respectively. Obviously, the finite-time control scheme can flexibly adjust the convergence time to improve the system performance.

References

1 Chen Y Y, Yu R, Zhang Y. Fully distributed spherical formation tracking control for nonlinear vehicles with spatiotemporal uncertainties and digraphs. Nonlinear Dyn, 2020, 101: 997–1013

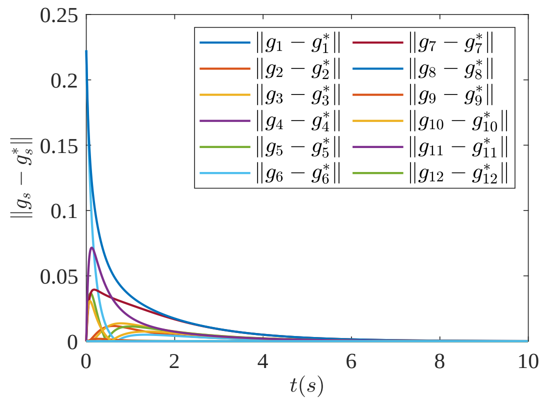

Figure F13 Bearing error with (F1) in Example 3.

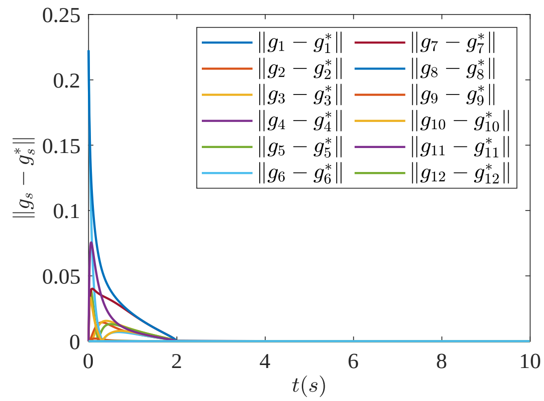

Figure F14 Bearing error with (D2) in Example 3.

2 Hacene N, Mendil B. Behavior-based autonomous navigation and formation control of mobile robots in unknown cluttered dynamic environments with dynamic target tracking. Int J Autom Comput, 2021, 18: 766–786

3 Savino H J, Pimenta L C, Shah J A, et al. Pose consensus based on dual quaternion algebra with application to decentralized formation control of mobile manipulators. Int J Autom Comput, 2020, 357: 142–178

4 Yu Y, Zeng Z, Li Z, et al. Event-triggered encirclement control of multi-agent systems with bearing rigidity. Sci China Inf Sci, 2017, 60: 1-18.

5 Briñón-Arranz L, Seuret A, Pascoal A. Circular formation control for cooperative target tracking with limited information. J Franklin Inst, 2019, 356: 1771–1788

6 Cheng B, Wu Z, Li Z. Distributed edge-based event-triggered formation control. IEEE Trans Cybernetics, 2019, 51: 1241–1252

7 Rozenheck O, Zhao S, Zelazo D. A proportional-integral controller for distance-based formation tracking. In: Proceedings of the 2015 European Control Conference (ECC), Austria, 2015. 1693–1698

8 Mehdifar F, Bechlioulis C P, Hashemzadeh F, et al. Prescribed performance distance-based formation control of multi-agent systems, Automatica, 2020, 119: 109086

9 Huang Y, Meng Z: Bearing-based distributed formation control of multiple vertical take-off and landing uavs. IEEE Trans Control Netw Syst, 2021, 8: 1281–1292

10 Trinh M H, Tran Q V, Vu D V, et al. Robust tracking control of bearing-constrained leader-follower formation. Automatica, 2021, 131: 109733

11 Zhao S, Zelazo D. Translational and scaling formation maneuver control via a bearing-based approach. IEEE Trans Control Netw Syst, 2015, 4: 429–438

12 Luo X, Li X, Li X, et al. Globally stable formation control of nonholonomic multiagent systems with bearing-only measurement. IEEE Syst J, 2019, 14: 2901–2912

13 Tron R, Thomas J, Loianno G, et al. A distributed optimization framework for localization and formation control: Applications to vision-based measurements. IEEE Control Syst Mag, 2016, 36: 22–44

14 Tang Z, Cunha R, Hamel T, et al. Relaxed bearing rigidity and bearing formation control under persistence of excitation. Automatica, 2022, 141: 110289

15 Li Z, Tnunay H, Zhao S, et al. Bearing-only formation control with prespecified convergence time. IEEE Trans Cybernetics, 2020, 52: 620–629

16 Tian J, Hu W. Bearing-only formation control of first-order discrete-time multi-agent systems. In: Proceedings of the 2021 11th International Conference on Information Science and Technology (ICIST), Chengdu, 2021. 466–470

17 Zhao S, Li Z, Ding Z. Bearing-only formation tracking control of multiagent systems. IEEE Trans Autom Control, 2019, 64: 4541–4554

18 Li X, Wen C, Chen C. Adaptive formation control of networked robotic systems with bearing-only measurements. IEEE Trans Cybernetics, 2020, 51: 199–209

19 Yang Z, Zhu S, Chen C, et al. Leader-follower formation control of nonholonomic mobile robots with bearing-only measurements. J Franklin Inst, 2020, 357: 1628–1643

20 Trinh M H, Oh K K, Jeong K, et al. Bearing-only control of leader first follower formations. IFAC-PapersOnLine, 2016, 49: 7–12

21 Zhao J, Yu X, Li X, et al. Bearing-only formation tracking control of multi-agent systems with local reference frames and constant-velocity leaders. IEEE Control Syst Lett, 2020, 5: 1–6

22 Trinh M H, Ahn H S. Finite-time bearing-based maneuver of acyclic leader-follower formations. IEEE Control Syst Lett, 2021, 6: 1004–1009

23 Xiong X, Yang X, Cao J, et al. Finite-time control for a class of hybrid systems via quantized intermittent control. Sci China Inf Sci, 2020, 63: 1-16.

24 Zhao J, Li X, Yu X, et al. Finite-time cooperative control for bearing-defined leader-following formation of multiple double-integrators. IEEE Trans Cybernetics, 2021, 52: 13363–13372

25 Li X, Zhu Y, Zhao X, et al. Bearing-based prescribed time formation tracking for second-order multi-agent systems. IEEE Trans Circuits Syst II Express Briefs, 2022, 69: 3259–3263

26 Trinh M H, Mukherjee D, Zelazo D, et al. Finite-time bearing-only formation control. In: Proceedings of the 2017 IEEE 56th Annual Conference on Decision and Control (CDC), Melbourne, 2017. 1578–1583

27 Van Tran Q, Trinh M H , Zelazo D, et al. Finite-time bearing-only formation control via distributed global orientation estimation. IEEE Trans Control Netw Syst, 2018, 6: 702–712

28 Wu K, Hu J, Lennox B, et al. Finite-time bearing-only formation tracking of heterogeneous mobile robots with collision

avoidance. IEEE Trans Circuits Syst II Express Briefs, 2021, 68: 3316–3320
29 Wang J L, Wu H N. Leader-following formation control of multi-agent systems under fixed and switching topologies. Int J Control, 2012, 85: 695–705
30 Wang Y, Cao J, Hu J. Pinning consensus for multi-agent systems with non-linear dynamics and time-varying delay under directed switching topology. IET Control Theory Appl, 2014, 8: 1931–1939
31 Li X, Yu Z, Li Z, et al. Group consensus via pinning control for a class of heterogeneous multi-agent systems with input constraints. Inf Sci, 2021, 542: 247–262
32 Zhao S, Zelazo D. Localizability and distributed protocols for bearing-based network localization in arbitrary dimensions. Automatica, 2016, 69: 334–341
33 Ji H, Yuan Q, Li C, et al. Bearing-only formation control of multi-agent system without leader's velocity information. IFAC-PapersOnLine, 2020, 53: 11044–11049